Human Adenovirus Infection Causes Cellular E3 Ubiquitin Ligase MKRN1 Degradation Involving the Viral Core Protein pVII

Raviteja Inturi,[a] Kwangchol Mun,[a] Katrin Singethan,[b] Sabrina Schreiner,[b] Tanel Punga[a]

[a]Department of Medical Biochemistry and Microbiology, Uppsala University, Uppsala, Sweden
[b]Institut für Virologie, Technische Universität München/Helmholtz Zentrum München, Munich, Germany

ABSTRACT Human adenoviruses (HAdVs) are common human pathogens encoding a highly abundant histone-like core protein, VII, which is involved in nuclear delivery and protection of viral DNA as well as in sequestering immune danger signals in infected cells. The molecular details of how protein VII acts as a multifunctional protein have remained to a large extent enigmatic. Here we report the identification of several cellular proteins interacting with the precursor pVII protein. We show that the cellular E3 ubiquitin ligase MKRN1 is a novel precursor pVII-interacting protein in HAdV-C5-infected cells. Surprisingly, the endogenous MKRN1 protein underwent proteasomal degradation during the late phase of HAdV-C5 infection in various human cell lines. MKRN1 protein degradation occurred independently of the HAdV E1B55K and E4orf6 proteins. We provide experimental evidence that the precursor pVII protein binding enhances MKRN1 self-ubiquitination, whereas the processed mature VII protein is deficient in this function. Based on these data, we propose that the pVII protein binding promotes MKRN1 self-ubiquitination, followed by proteasomal degradation of the MKRN1 protein, in HAdV-C5-infected cells. In addition, we show that measles virus and vesicular stomatitis virus infections reduce the MKRN1 protein accumulation in the recipient cells. Taken together, our results expand the functional repertoire of the HAdV-C5 precursor pVII protein in lytic virus infection and highlight MKRN1 as a potential common target during different virus infections.

IMPORTANCE Human adenoviruses (HAdVs) are common pathogens causing a wide range of diseases. To achieve pathogenicity, HAdVs have to counteract a variety of host cell antiviral defense systems, which would otherwise hamper virus replication. In this study, we show that the HAdV-C5 histone-like core protein pVII binds to and promotes self-ubiquitination of a cellular E3 ubiquitin ligase named MKRN1. This mutual interaction between the pVII and MKRN1 proteins may prime MKRN1 for proteasomal degradation, because the MKRN1 protein is efficiently degraded during the late phase of HAdV-C5 infection. Since MKRN1 protein accumulation is also reduced in measles virus- and vesicular stomatitis virus-infected cells, our results signify the general strategy of viruses to target MKRN1.

KEYWORDS adenoviruses, proteasome, ubiquitination

Human adenoviruses (HAdVs) are common pathogens, and their infections cause a wide range of diseases, including respiratory illness, keratoconjunctivitis, and gastroenteritis (1, 2). HAdVs are nonenveloped viruses with a linear double-stranded DNA genome embedded in a protective viral core structure. Inside the core, HAdV DNA associates with the viral proteins V, VII, Mu, terminal protein, and DNA-dependent adenovirus proteinase (Avp) (3). Protein VII is expressed during the late phase of infection, and it accumulates as a precursor polypeptide, designated the pVII protein (4). Precursor pVII protein undergoes site-specific Avp-dependent cleavage to form mature VII protein during the final steps of virus maturation (5–9). This proteolytic

cleavage step ensures proper condensation of viral DNA and proteins within the HAdV core (10, 11). Avp cleavage may also control protein stability, since unlike precursor pVII, mature VII is resistant to proteasomal degradation by cellular Cullin-3-based E3 ubiquitin ligase complexes (12).

Due to its histone-like characteristics, mature VII protein is able to assemble viral DNA into nucleosome-like structures (11, 13–16). Although protein VII is not required to condense viral DNA within the capsid, lack of it blocks productive virus infection (17). Several functions have been assigned to protein VII due to its interaction with DNA. Mature protein VII promotes nuclear import of viral DNA (18–20) and protects incoming viral DNA from the cellular DNA damage response (21). Protein VII can also introduce changes into the virus genome structure. This involves the gradual loss of mature VII protein from virus DNA during the transition from the early to the late phase of infection. Here, the reduced VII binding correlates with increased nucleosomal histone accumulation on viral DNA (22, 23). Protein VII can also recruit cellular template activating factor TAF-1β (also known as SET) to remodel the virus genome and to increase accessibility to transcription factors (24–26). Since protein VII interacts with DNA, it can have both negative and positive effects on target gene expression (22, 27). In addition to viral DNA, mature protein VII also associates with host cell chromatin. By binding to cellular nucleosomes, mature VII alters the cellular HMGB1 and HMGB2 protein functions on the host cell chromatin and thereby suppresses cellular inflammatory signaling (28). Binding of mature VII to cellular chromatin can also inhibit the DNA damage response on the host genome (29).

Covalent attachment of the ubiquitin moiety by the E3 ubiquitin ligases to substrate proteins can lead to proteolytic degradation via the ubiquitin-proteasome system (UPS) (30). Viruses, such as HAdV, often target the UPS to achieve efficient replication in host cells (reviewed in references 31, 32 and 33). This is exemplified by HAdV E1B55K/E4orf6 protein complexes, which by recruiting Cullin-based E3 ubiquitin ligases, promote proteasomal degradation of the cellular p53, Mre11, DNA ligase IV, integrin α3, Tip60, ATRX, Daxx, and SPOC1 proteins (34–40).

The Makorin ring finger protein 1 (MKRN1) gene was first reported as an intron-containing source gene for the Makorin ring finger (MKRN) gene family. The conserved MKRN1protein contains several zinc finger motifs and a single RING finger domain (41). MKRN1 functions as an E3 ubiquitin ligase since it contains a functional RING finger domain at the C terminus of the protein (42). Several cellular proteins, including hTERT, p53, p21, PPARγ, p14ARF, FADD, and PTEN, are known substrates for MKRN1-mediated ubiquitination and proteasomal degradation (42–47). Viral proteins, such as West Nile virus (WNV) and porcine circovirus type 2 (PCV2) capsid proteins, also interact with MKRN1 (48, 49). Only WNV capsid protein (WNVCp) has been shown to be ubiquitinated and degraded by the proteasome in a MKRN1-dependent manner (48). The MKRN1 protein has also been characterized as an RNA-binding protein with potential to regulate RNA metabolism in mouse embryonic stem cells (50). Further, MKRN1 can repress transcription on different cellular promoters independently of its described E3 ligase activity (46, 51).

Even though protein VII has been extensively characterized as a virus DNA-binding protein, not much is known about its interactions with cellular proteins. Considering its essential role during productive infection (17), it is reasonable to assume that protein VII interacts with a variety of cellular proteins. This study was undertaken to identify novel precursor pVII-interacting proteins and to elucidate the functional consequences of these interactions.

RESULTS

Identification of precursor pVII-interacting proteins. To identify cellular proteins specifically interacting with HAdV-C5 precursor pVII protein, we performed a yeast two-hybrid (Y2H) screening experiment. The precursor pVII protein [here referred to as pVII(wt)] was used as the bait to screen the human lung cancer cell line cDNA library. Sequencing of the cDNA clones identified 13 potential proteins interacting with the

TABLE 1 Identified precursor pVII-interacting proteins in yeast two-hybrid screen

Official gene symbol	Official full name	Gene ID	No. of clones	PBS[a]
C1QBP	Complement C1q binding protein	708	100	A
SET	SET nuclear proto-oncogene	6418	36	A
HMGB2	High mobility group box 2	3148	30	A
HMGB3	High mobility group box 3	3149	13	A
SETSIP	SET-like protein	646817	15	B
ZNF622	Zinc finger protein 622	90441	4	C
CHD3	Chromodomain helicase DNA binding protein 3	1107	4	D
MKRN1	Makorin ring finger protein 1	23608	2	D
BAZ1A	Bromodomain adjacent to zinc finger domain 1A	11177	1	D
CTPS1	CTP synthase 1	1503	1	D
RACK1	Receptor for activated C kinase 1	10399	1	D
PTGES3L-AARSD1	PTGES3L-AARSD1 readthrough	100885850	1	D
ARMCX2	Armadillo repeat containing, X-linked 2	9823	1	D

[a]PBS, predicted biological score.

precursor pVII protein (Table 1). The identified proteins were further grouped based on their predicted biological score (PBS; see Materials and Methods). The proteins having the highest number of clones and the best PBS score were C1QBP, SET, HMGB2, and HMGB3. In addition, the Y2H screen recovered clones with lower PBS scores, such as SETSIP, ZNF622, CHD3, MKRN1, BAZ1A, CTPS1, and RACK1. The specificity of our Y2H screen was strengthened by the observation that the SET, HMGB2, and HMGB3 proteins have been previously shown to bind mature VII protein [here referred to as pVII(Δ24)] in HAdV-infected cells (28, 52). To validate the Y2H screen results, we performed a proximity ligation assay (PLA) in HeLa cells expressing the precursor pVII-Flag protein [here referred to as pVII(wt)-Flag] after doxycycline treatment. PLA was performed with antibodies against some of the identified proteins (Table 1) and with an anti-Flag-antibody to detect protein-protein interactions in cells. All the tested proteins showed detectable proximity ligation in the pVII(wt)-Flag protein-expressing cells (Fig. 1). Further quantification confirmed that proximity ligation of the HMGB2, C1QBP, MKRN1, SET, BAZ1A, and CHD3 proteins with pVII(wt)-Flag protein was above the background signal obtained with an irrelevant antibody in the control reaction.

Since pVII(wt) protein stability can be controlled by the UPS (12), we concentrated our efforts on the identified E3 ubiquitin ligase MKRN1 and its interference with the pVII(wt) protein.

Precursor pVII protein interacts with MKRN1 in HAdV-C5-infected cells. To study whether MKRN1 interacts with pVII(wt) during HAdV-C5 infection, we generated a replication-competent HAdV-C5 virus expressing Flag epitope-containing pVII protein (here referred to as HAdV-pVII-Flag). This virus was used to infect H1299 cells, followed by immunoprecipitation of the pVII(wt)-Flag protein 20 h postinfection (hpi). The results confirmed that pVII(wt)-Flag interacts with the endogenous MKRN1 protein in virus-infected cells and that this interaction was enhanced in the presence of proteasome inhibitor MG132 (Fig. 2A, lanes 4 to 6). To show the assay specificity, we confirmed that pVII(wt)-Flag interacted with HMGB2, a previously established protein VII interactor (28) (Fig. 2A, WB:HMGB2). In contrast, an abundant HAdV-C5 early protein, E1A, did not show detectable binding to the pVII-Flag protein in our experimental system (Fig. 2A, WB:E1A). Both precursor pVII [pVII(wt)] and mature VII [pVII(Δ24)] (12) proteins are present in HAdV-C5-infected cells (53). Mature VII is generated from precursor pVII after Avp proteolytic cleavage of the propeptide module (7, 8). To study if the propeptide module (amino acids 1 to 24 in HAdV-C5) influences the precursor pVII protein binding to MKRN1, we performed coimmunoprecipitation experiments with H1299 cell lysates expressing the pVII(wt)-Flag or pVII(Δ24)-Flag proteins in the presence of hemagglutinin-tagged MKRN1(wt) [HA-MKRN1(wt)]. As shown in Fig. 2B, the lack of a propeptide sequence in pVII(Δ24) reduced the protein binding to HA-MKRN1(wt) (lanes 5 and 6). A similar result was observed with the glutathione S-transferase (GST) pulldown experiment, in which GST-pVII(Δ24) showed reduced
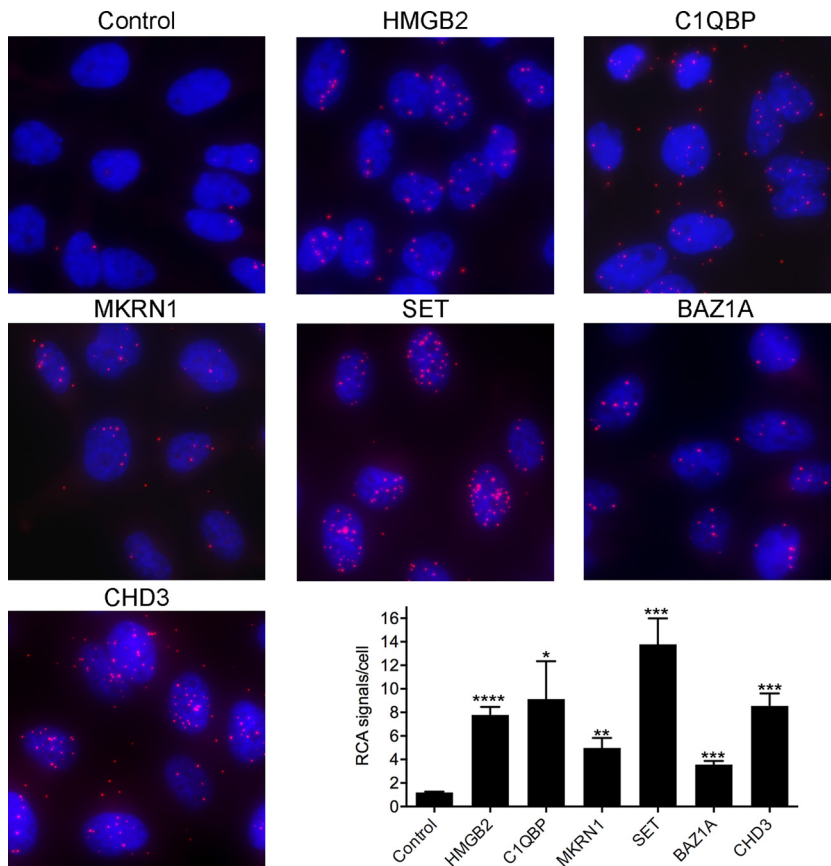
FIG 1 Proximal association of the precursor pVII(wt)-Flag protein and its interacting proteins. A proximity ligation assay (PLA) was performed in a stable HeLa cell line expressing the pVII(wt)-Flag protein after doxycycline treatment. The proteins analyzed for pVII(wt)-Flag binding are shown above the images. In the control reaction, an irrelevant antibody (anti-HA) was used. Proximity ligation signals were amplified with rolling circle amplification (RCA) and are shown in red, whereas blue is Hoechst dye staining the nuclei. Quantification of the proximity ligation event is shown as the number of RCA signals/cell, analyzed in triplicate. Bars denote the mean number of RCA signals ($\pm$SD)/cell. An unpaired t test indicated significantly (****, $P < 0.0001$; ***, $P < 0.001$; **, $P < 0.01$; *, $P < 0.05$) higher numbers of RCA signals/cell in specific antibody samples than in the control (anti-HA) sample.

binding to Flag-MKRN1 compared to GST-pVII(wt) (Fig. 2C). In order to identify which region(s) of the MKRN1 protein interacts with pVII, different HA-tagged MKRN1 deletion mutant proteins were constructed (Fig. 2D). The GST pulldown experiment with H1299 cell lysates expressing the HA-MKRN1 proteins revealed that both N-terminal (amino acids 1 to 267) and C-terminal (amino acids 112 to 482) MKRN1 regions were able to bind to GST-pVII(wt) (Fig. 2E). Since the HA-MKRN1(112-267) protein was deficient in binding to pVII (Fig. 2E, lane 11), it is likely that HA-MKRN1 regions comprising amino acids 1 to 111 and 268 to 482 provide an interaction surface for the pVII(wt) protein.

MKRN1 protein undergoes proteasomal degradation in HAdV-C5-infected cells. Since HAdV infections cause proteasomal degradation of several host proteins (reviewed in references 31, 32, and 33), it became of interest to evaluate the steady-state level of the endogenous MKRN1 protein in HAdV-C5-infected cells. H1299 cells were infected with HAdV-C5, and the endogenous MKRN1 protein was monitored during a 48-h infection time course. The MKRN1 protein was undetectable from 20 hpi onwards, overlapping with virus capsid protein accumulation in the infected H1299 cells (Fig. 3A). To establish if the MKRN1 protein disappearance was due to its proteasomal degradation, HAdV-C5-infected H1299 cells were treated with MG132. The MKRN1 protein levels were restored in the MG132-treated cells (Fig. 3B, lanes 3 and 4),
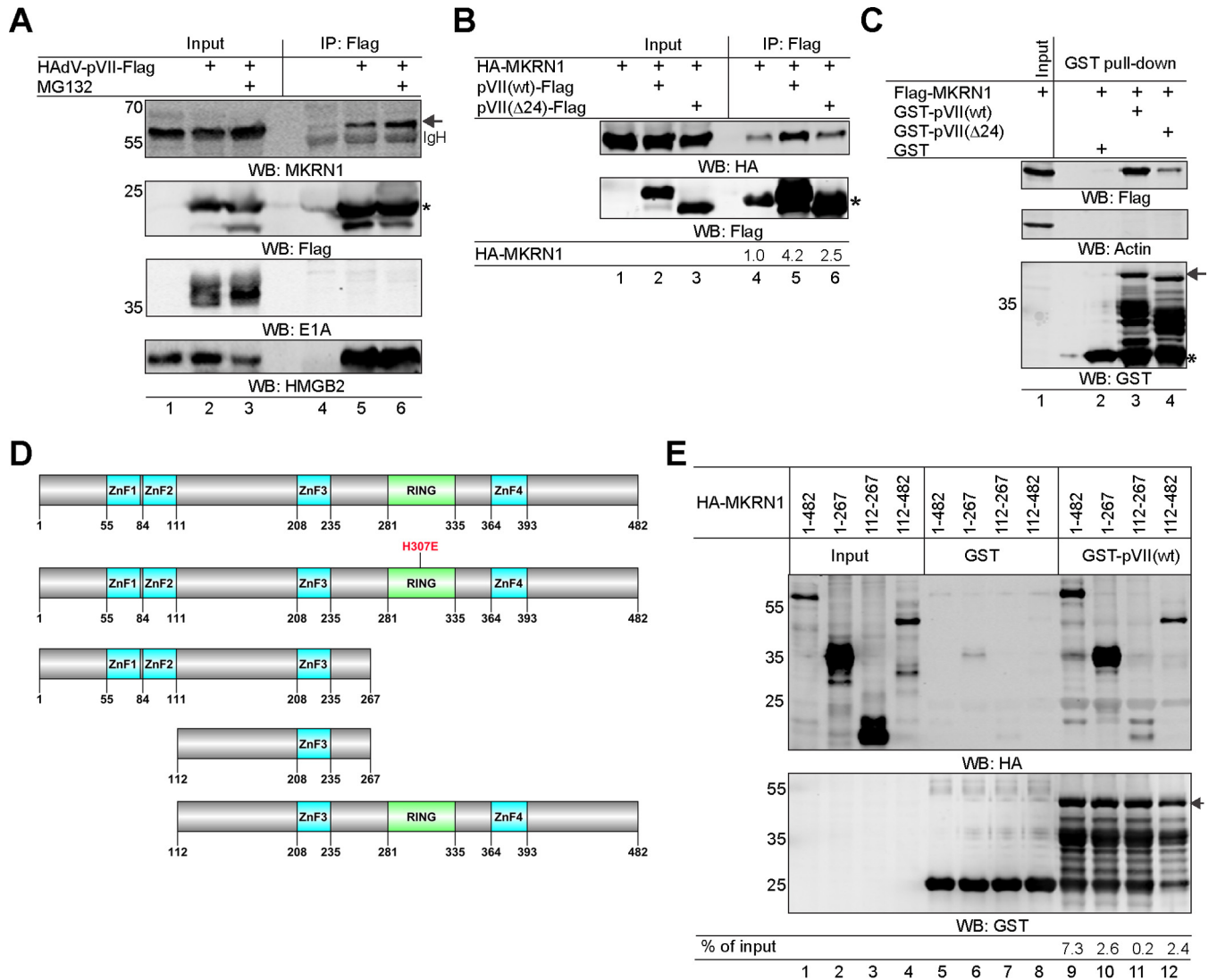
FIG 2 The precursor pVII protein interacts with MKRN1 *in vitro* and *in vivo*. (A) H1299 cells were infected with HAdV-pVII-Flag virus (5 FFU/cell) for 20 h, followed by immunoprecipitation (IP) with an anti-Flag antibody (lanes 2 and 5). Cells were treated with MG132 (4 h, 25 μM) at 16 hpi and collected at the same time as the non-MG132-treated cells (lanes 3 and 6). Detection of the HAdV-C5 E1A and cellular HMGB2 proteins was used as the specificity control. An arrow points to migration of the MKRN1 protein, while an asterisk indicates migration of the pVII-Flag protein. WB, Western blotting. (B) H1299 cell lysates transiently expressing the HA-MKRN1(wt) and pVII(wt)-Flag or pVII(Δ24)-Flag proteins were immunoprecipitated with an anti-Flag antibody. Relative binding levels of HA-MKRN1 from two independent experiments are shown below the image after normalization to the input values. An asterisk indicates migration of the Flag antibody light chain. Note that HA-MKRN1 has some unspecific binding to Flag-coupled beads (lane 4). (C) GST-pVII(wt) and GST-pVII(Δ24) pulldown experiment with H1299 whole-cell lysates expressing the Flag-MKRN1(wt) protein. An arrow indicates migration of full-length GST-pVII proteins, while an asterisk marks migration of the GST protein. (D) Illustration of the MKRN1 mutant proteins. Labeling of zinc finger motifs (ZnF) and RING finger (RING) domain is based on Uniprot (www.uniprot.org) annotation. (E) GST-pVII(wt) pulldown experiment with H1299 whole-cell lysates expressing the indicated HA-MKRN1 proteins. Quantitative binding levels of the respective HA-MKRN1 proteins to GST-pVII(wt) are shown after normalization to input values (% of input). An arrow indicates migration of the GST-pVII(wt) protein.

indicating that the protein undergoes proteasomal degradation in HAdV-C5-infected cells. This is further supported by the observation that MKRN1 mRNA accumulation was not affected in infected H1299 cells (Fig. 3C). To test if the observed MKRN1 disappearance correlated with the accumulation of the pVII protein during infection, H1299 cells were infected with the HAdV-pVII-Flag virus. As shown in Fig. 3D, expression of pVII from 16 hpi onwards correlated with reduced accumulation of the MKRN1 protein. The disappearance of MKRN1 was not H1299 cell line specific, since a similar effect was observed in HAdV-C5-infected A549, U2OS, and HEK293 cell lines (Fig. 3E). Taken together, our results indicate that MKRN1 undergoes proteasomal degradation during the late phase of infection in various HAdV-C5-infected cell lines.
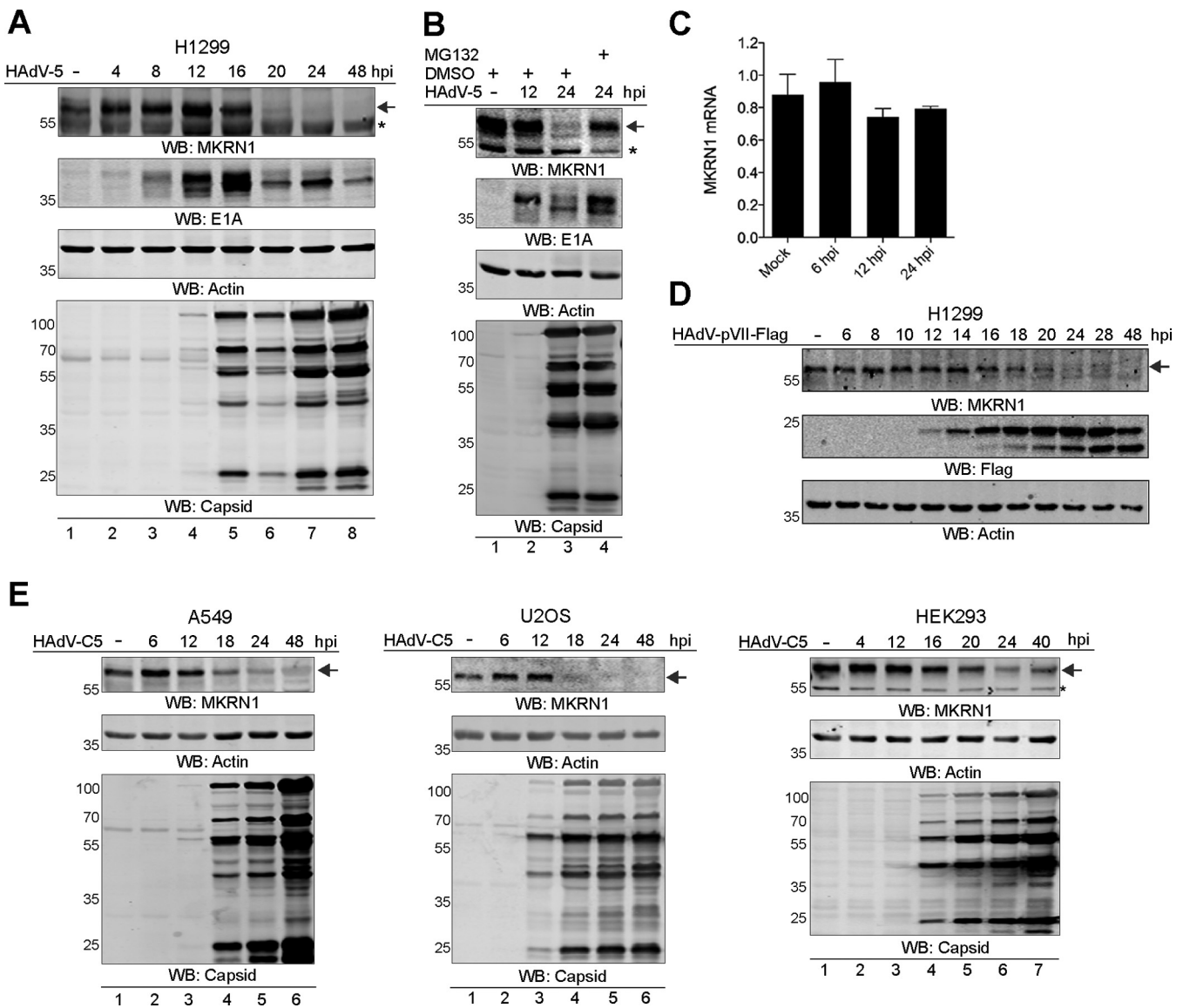
FIG 3 The MKRN1 protein undergoes proteasomal degradation in HAdV-C5-infected cells. (A) H1299 cells were infected with HAdV-C5 (10 FFU/cell). Whole-cell lysates were collected at the indicated hours postinfection (hpi) and analyzed by WB. An arrow indicates migration of MKRN1, while an asterisk marks an unspecific protein occasionally detected with MKRN1 antibody. (B) HAdV-C5-infected (10 FFU/cell) H1299 cells were treated at 20 hpi with MG132 (4 h, 25 μM). All cell samples were harvested 24 hpi and analyzed by WB. Detection of the HAdV-C5 E1A protein acts as a positive control for MG132 treatment. (C) H1299 cells were infected with HAdV-C5 (10 FFU/cell) for the indicated time points. Relative MKRN1 mRNA expression levels were analyzed by qRT-PCR after normalization to HPRT1 mRNA. Bars denote the mean ± SD MKRN1 expression levels. (D) H1299 cells were infected with HAdV-pVII-Flag virus (10 FFU/cell) and harvested at the indicated hours postinfection. Expression of the HAdV-encoded pVII-Flag was detected with an anti-Flag antibody. (E) A549, U2OS, and HEK293 cells were infected with HAdV-C5 (10 FFU/cell), harvested at the indicated hours postinfection, and analyzed for protein expression as described for panels A and D.

MKRN1 protein degradation is independent of the E1B55K and E4orf6 proteins. HAdVs encode the E1B55K and E4orf6 proteins, which by binding to Cullin-based E3 ubiquitin ligases induce proteasomal degradation of cellular proteins in infected cells. To investigate whether MKRN1 degradation is dependent on the E1B55K and E4orf6 proteins, Flag-tagged versions of both proteins were transiently overexpressed in H1299 cells. As shown in Fig. 4A, endogenous MKRN1 was not affected by expression of the Flag-E1B55K and/or Flag-E4orf6 proteins. In the same experiment, a well-known E1B55K/E4orf6 target protein, Mre11 (40), was downregulated (Fig. 4A, lanes 4 and 8; see also the quantification). To further demonstrate that proteasomal degradation of MKRN1 occurs independently of the E1B55K/E4orf6 complex, H1299 cells were infected with wild-type HAdV-C5 and E1B55K-deleted dl1520 virus (54). The MKRN1 protein
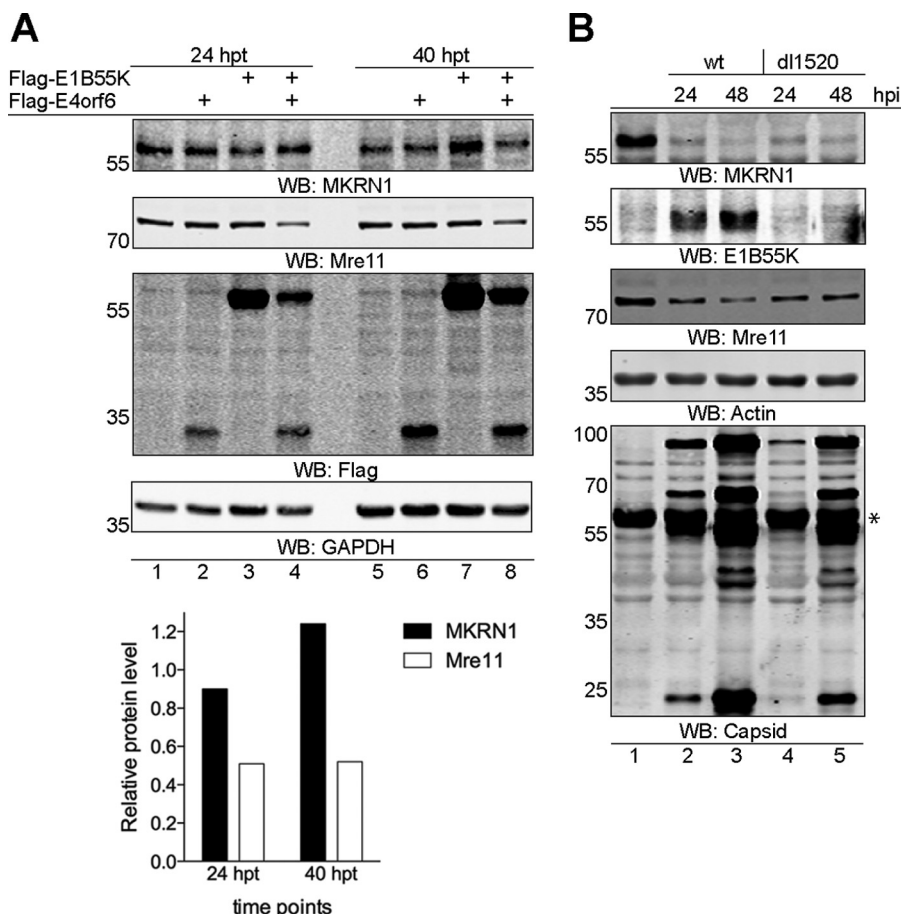
FIG 4 The MKRN1 protein is degraded independently of the E1B55K and E4orf6 proteins. (A) H1299 cells were transiently transfected with plasmids expressing the Flag-E1B55K and/or Flag-E4orf6 proteins. Whole-cell extracts were made at the indicated hours posttransfection (hpt), and proteins were detected by WB. Detection of the Mre11 protein was used to confirm the functionality of the E1B55K/E4orf6 complex. Relative quantification of the Mre11 and MKRN1 proteins in Flag-E1B55K- and Flag-E4orf6-expressing cells (lanes 4 and 8) compared to control transfected cells (lanes 1 and 5) is shown on the graph below the WB images. The Mre11 and MKRN1 protein levels were normalized to GAPDH protein. (B) H1299 cells were infected (10 FFU/cell) with HAdV-C5 (wt) and HAdV-C2 (dl1520) viruses. Whole-cell lysates were analyzed by WB at 24 and 48 hpi. An asterisk denotes an unspecific protein recognized with the anti-capsid antibody after WB membrane stripping.

levels were reduced by both virus infections, whereas the Mre11 protein was affected only in wild-type virus-infected cells (Fig. 4B). Taken together, our data suggest that proteasomal degradation of MKRN1 in HAdV-infected cells occurs independently of the E1B55K/E4orf6 protein complex.

pVII(wt) protein enhances MKRN1 protein self-ubiquitination. MKRN1 protein binds to the substrate proteins via the C-terminal RING finger domain to promote target protein ubiquitination and proteasomal degradation (42, 48). In addition, MKRN1 undergoes self-ubiquitination and proteasomal degradation, which may control its activity in cells (42, 55). Since pVII(wt) interacts with MKRN1 via the RING finger domain (Fig. 2E), our initial logical follow-up was to test whether the pVII(wt) protein was ubiquitinated in an MKRN1-dependent manner. Despite several attempts, we were unable to detect MKRN1-dependent pVII(wt) ubiquitination (data not shown). The observation that pVII(wt) also binds to the N-terminal part of MKRN1 (Fig. 2E) urged us to test whether this viral protein has any impact on the MKRN1 E3 ubiquitin ligase activity. Expression of the precursor pVII(wt)-Flag protein enhanced MKRN1 ubiquitination in His-ubiquitin-expressing H1299 cells when analyzed with a nickel pulldown experiment (Fig. 5A, lanes 2 and 3). Enhanced MKRN1 ubiquitination was specific to the
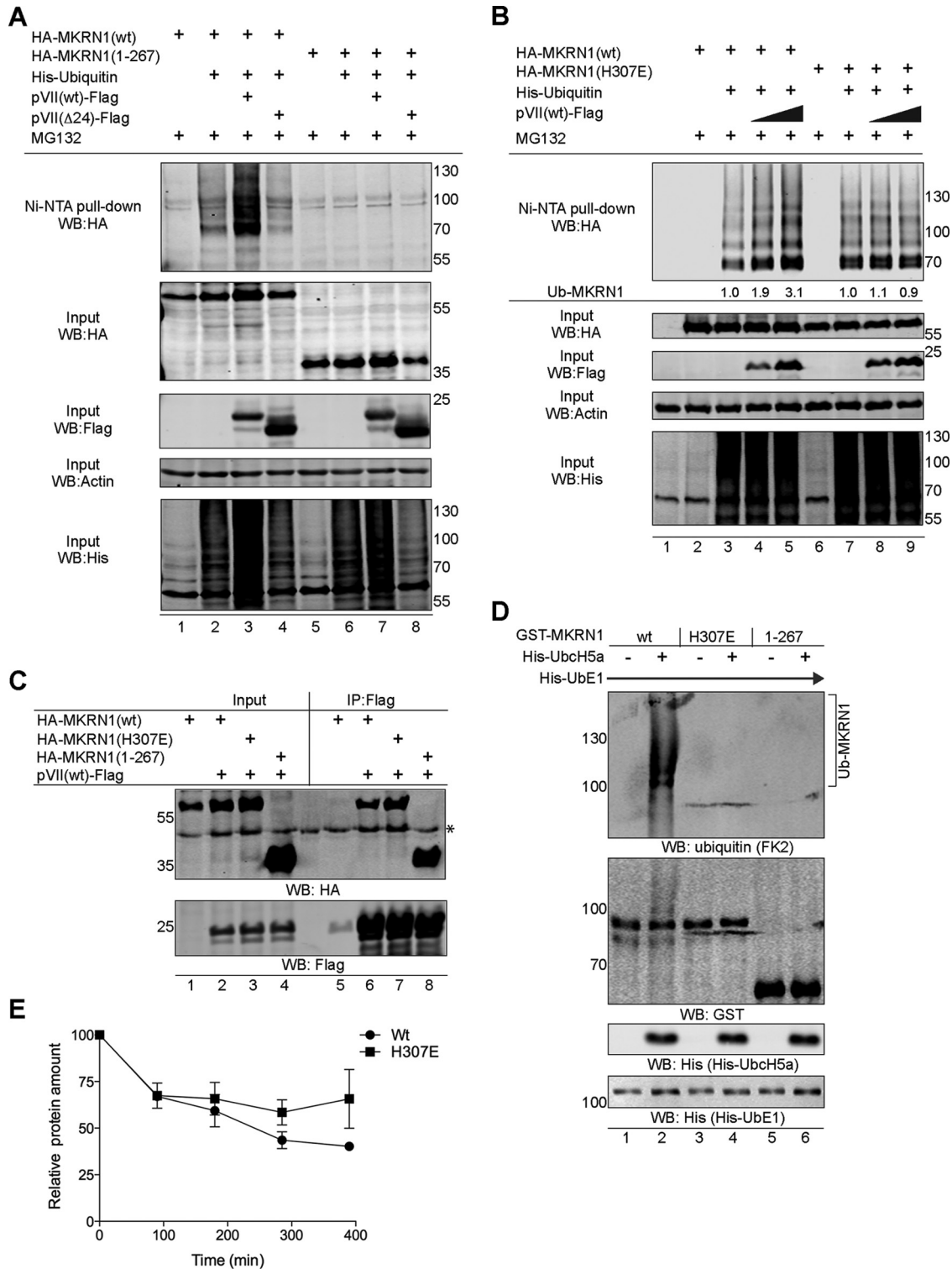
FIG 5 The precursor pVII protein enhances MKRN1 self-ubiquitination. (A) pVII(wt)-Flag enhances MKRN1 ubiquitination *in vivo*. H1299 cells were transfected with plasmids expressing the 6×His-ubiquitin, HA-MKRN1 (wt or 1-267), pVII-Flag (wt or Δ24) proteins. Cells were treated 36 hpt with MG132 (10 μM, 4 h). Ubiquitinated proteins were isolated using the nickel pulldown (Ni-NTA) approach and analyzed along with the whole-cell lysate input samples by WB. (B) MKRN1(H307E) is resistant to pVII(wt) enhanced ubiquitination. Ni-NTA pull down was done in H1299 cells expressing HA-MKRN1(wt or H307E), pVII(wt)-Flag, and 6×His-ubiquitin proteins. Cells were harvested and treated as described for panel A. Ubiquitin signals were quantitated, and the relative level of HA-MKRN1-coupled His-ubiquitin (Ub-MKRN1) is shown below the first panel ("Ni-NTA pull-down WB:HA"). (C) The pVII(wt)-Flag protein coimmunopre-cipitates with HA-MKRN1 (wt, H307E, and 1-267) in transiently transfected H1299 cells. An asterisk indicates detection of unspecific protein with an anti-HA antibody. (D) MKRN1(H307E) is deficient in self-ubiquitination. An *in vitro* ubiquitination assay was performed with the indicated recombinant His- and GST-tagged proteins in the presence of purified ubiquitin protein. Ubiquitinated GST-MKRN1

(Continued on next page)

pVII(wt)-Flag protein, since basal MKRN1 ubiquitination remained the same in cells expressing the mature VII [pVII(Δ24)] protein (Fig. 5A, lanes 2 and 4). The inability of pVII(Δ24) to enhance MKRN1 ubiquitination is probably due to reduced binding of the pVII(Δ24) protein to MKRN1 (Fig. 2B and C). Further, the specificity of the experiment was confirmed by the lack of ubiquitination in cells expressing the MKRN1(1-267) protein (Fig. 2D), which lacks the RING finger domain (Fig. 5A, lanes 5 to 8). Previous studies have shown that mutation of the histidine residue at position 307 (H307E) in the RING finger domain (Fig. 2D) blocks MKRN1's ability to ubiquitinate the substrate proteins (42, 46). The MKRN1(H307E) protein itself was ubiquitinated in our *in vivo* ubiquitination experiment in H1299 cells (Fig. 5B, lanes 3 and 7), suggesting that MKRN1(H307E) can serve as a substrate for ubiquitination. In contrast to HA-MKRN1(wt) (Fig. 5B, lanes 3 to 5), ubiquitination of the HA-MKRN1(H307E) protein was not enhanced by the pVII(wt)-Flag protein (Fig. 5B, lanes 7 to 9). This discrepancy was not due to different affinities of the MKRN1 proteins, as both HA-MKRN1(wt) and HA-MKRN1(H307E) bound equally well to pVII(wt)-Flag (Fig. 5C). The observation that MKRN1(H307E) was ubiquitinated in our experiments urged us to further study the details of this particular mutation. We performed *in vitro* ubiquitination experiments with the purified E1 (His-UbE1), E2 (His-UbcH5a), and E3 (GST-MKRN1) proteins, which revealed that the MKRN1(H307E) protein is defective in self-ubiquitination (Fig. 5D, lanes 2 and 4). Since the pVII(wt) protein did not promote MKRN1(H307E) self-ubiquitination (Fig. 5B), we hypothesized that this mutant protein might be more stable in HAdV-C5-infected cells than the wild-type protein. To test this hypothesis, we infected H1299 cells expressing either the HA-MKRN1(wt) or HA-MKRN1(H307E) protein with HAdV-pVII-Flag virus and blocked *de novo* protein synthesis with cycloheximide. As shown in Fig. 5E, the HA-MKRN1(wt) protein showed faster decay in the presence of cycloheximide than the HA-MKRN1(H307E) protein, suggesting that the latter is resistant to proteasomal degradation in virus-infected H1299 cells. Collectively, our data indicate that pVII(wt), but not pVII(Δ24), enhances MKRN1 protein self-ubiquitination.

Downregulation of MKRN1 is not limited to HAdV-C5 infection. Considering the effective elimination of MKRN1 in HAdV-C5-infected cells (Fig. 3), we hypothesized that MKRN1 might also be affected in cells infected with other pathogenic viruses. Therefore, we analyzed MKRN1 accumulation in permissive cells infected with human immunodeficiency virus type 1 (HIV-1), hepatitis C virus (HCV), measles virus (MV), vesicular stomatitis virus (VSV), and hepatitis B virus (HBV). The MKRN1 protein levels were reduced in MV- and VSV-infected cells, whereas HIV-1, HCV, and HBV infections did not considerably affect the MKRN1 protein levels (Fig. 6).

DISCUSSION

The HAdV mature VII protein has long been considered a virus genome organizing factor (14). Although mature VII is not required to condense DNA within the capsid, it is essential for productive infection (17). The present study and the recent elegant reports from the Weitzman (28, 29) and Hearing (17) laboratories are the latest progressive attempts to elucidate the important functions of pVII protein in HAdV-infected cells.

In this report, we aimed to identify novel precursor pVII(wt)-interacting proteins and to relate the identified interactors with yet uncharacterized functions of the pVII protein. We found that the pVII(wt) protein interacts with the CHD3 and BAZ1A proteins (Table 1 and Fig. 1), which are both involved in chromatin remodeling (56, 57). Considering the reported activities of protein VII on gene expression (22, 27) and

FIG 5 Legend (Continued)

(Ub-MKRN1) was detected with an anti-ubiquitin (FK2) antibody. (E) MKRN1(H307E) degradation is decelerated in virus-infected cells. H1299 cells were transiently transfected with plasmids expressing the HA-MKRN1(wt) or HA-MKRN1(H307E) proteins, followed by HAdV-pVII-Flag infection (2 FFU/cell). Cells were treated at 48 hpi with cycloheximide, and whole-cell lysates were prepared from cells harvested at 90, 180, 285, and 390 min posttreatment. The HA-tagged MKRN1 and actin proteins were quantified on WB, and the relative HA-MKRN1 protein levels were calculated after normalization to actin. The mean ± SEM of results from two independent experiments is shown.
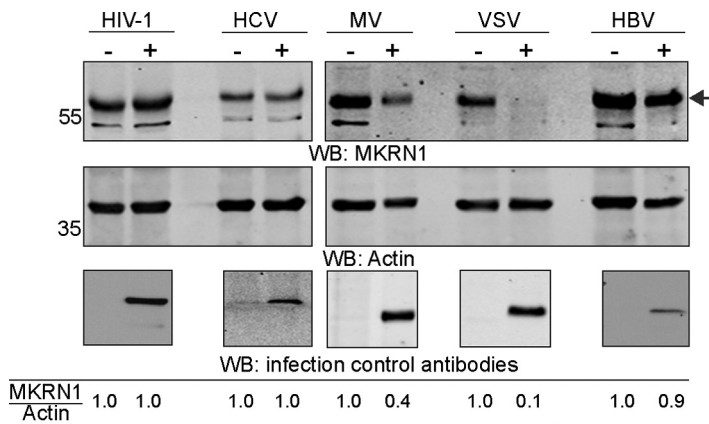
FIG 6 MKRN1 protein accumulation is downregulated in VSV- and MV-infected cells Total protein lysates of cells either infected (+) or noninfected (−) with the indicated viruses were analyzed by WB. An arrow indicates migration of the endogenous MKRN1 protein. Relative accumulation of the MKRN1 protein is shown after normalization to actin (MKRN1/Actin). Virus infections were confirmed with the following antibodies: anti-p24 (HIV-1), anti-core (HCV), anti-nucleoprotein NP (MV), anti-GFP (VSV), and anti-core (HBV). HCV, MV, and VSV infections were confirmed on the same WB membrane as the MKRN1 and actin proteins, whereas HIV-1 and HBV infections were confirmed on a separate WB membrane.

chromatin structure regulation (13, 15, 28), it is theoretically possible that the interaction of pVII(wt) with the CHD3 and BAZ1A proteins is needed to achieve optimal pVII-dependent chromatin remodeling in HAdV-infected cells. In addition, we identified two other chromatin structure-regulating proteins, HMGB2 and HMGB3, as the pVII(wt)-interacting proteins. This finding is in line with a recent report in which mature protein VII was shown to interact with the HMGB1, HMGB2, and HMGB3 proteins in A549 cells (28). Even though mature protein VII impacts antiviral responses by altering the HMGB1 and HMGB2 protein functions on the host cell chromatin, the functional impact of the pVII(wt) protein on HMGB3 remains to be tested.

One of the identified pVII(wt)-interacting proteins in the Y2H screen was the E3 ubiquitin ligase MKRN1 (Table 1). Since we have previously shown that the precursor pVII protein is targeted for proteasomal degradation (12), we hypothesized that MKRN1 might be the E3 ubiquitin ligase mediating pVII(wt) ubiquitination and its subsequent proteasomal degradation. Even though MKRN1 transient overexpression reduced pVII(wt) protein levels in a proteasome-dependent manner, we were unable to confirm that the pVII(wt) protein was directly ubiquitinated by MKRN1 (data not shown). Instead, our detailed analysis revealed that MKRN1 undergoes proteasomal degradation during the late phase of infection in various human cell lines (Fig. 3). In this regard, MKRN1 degradation in HAdV-C5-infected cells is unusual, since it does not rely on the E1B55K and E4orf6 proteins (Fig. 4), which are well-characterized viral proteins targeting multiple cellular proteins for proteasomal degradation in HAdV-infected cells (31–33). Based on our protein-protein interaction experiments and observation that MKRN1 degradation correlated with the onset of the HAdV late protein accumulation (Fig. 2 and 3), we hypothesized that the pVII(wt) protein might be involved in MKRN1 stability regulation. Previous studies have revealed that MKRN1 interacts with its target proteins, such as p53 and WNVCp, via the C-terminal RING finger domain to ensure substrate protein ubiquitination and subsequent proteasomal degradation (46, 48). Our observation that pVII(wt) interacts with both MKRN1 N- and C-terminal regions suggests that pVII(wt) interference with MKRN1 may not follow a typical enzyme-substrate interaction leading to a substrate protein, such as pVII(wt), ubiquitination and degradation. This was supported by the observation that the precursor pVII protein enhanced MKRN1 self-ubiquitination, whereas the mature VII, which showed reduced binding to MKRN1, was deficient in this function (Fig. 5A and B). Therefore, we propose a model in which during the late phase of infection the precursor pVII protein saturates both the N- and C-terminal binding sites on MKRN1, which in turn leads to MKRN1 self-

ubiquitination. This dual binding mode may be due to the increased pVII(wt) protein concentration during the late phase of infection. Alternatively, since the pVII protein is extensively modified by phosphorylation and acetylation (28, 58), it is possible that these posttranslational modifications increase pVII(wt) affinity toward MKRN1. Our model suggests that precursor pVII may display separate functions from mature VII. This novel function assigned to precursor pVII may explain why the cleavage of the propeptide module occurs only during the final steps of virus particle maturation. Hypothetically, early cleavage of the precursor pVII to mature VII protein will not cause MKRN1 proteasomal degradation, since the mature VII is deficient in promoting MKRN1 self-ubiquitination. Although the precursor pVII induces MKRN1 self-ubiquitination, expression of pVII(wt) alone, outside the virus infection context, was not sufficient to cause MKRN1 proteasomal degradation (data not shown). This observation implies that even though the precursor pVII protein enhances MKRN1 self-ubiquitination, there is a need for an additional, yet unknown factor in HAdV-C5-infected cells to achieve MKRN1 proteasomal degradation.

We also found that two other pathogenic viruses, MV and VSV, affected MKRN1 protein accumulation in their respective recipient cells (Fig. 6). Three different virus infections (HAdV-C5, MV, and VSV infections) downregulate MKRN1 protein accumulation (present study), and at least two other viruses (WNV, PCV2) encode the proteins interacting with MKRN1 (48, 49). Further, the observation that MKRN3 restricts HIV-1 infection in human cells may indicate the involvement of different MKRN gene family members in controlling virus infections (59). This broad targeting raises an important question as to why different viruses impede MKRN1 functions. It is theoretically possible that downregulation of the MKRN1 protein is beneficial for optimal virus growth, since MKRN1 may affect viral protein ubiquitination, gene transcription, and RNA metabolism. Further studies are needed to reveal the exact role of the MKRN1 protein and its family members in various virus infections.

In conclusion, our novel findings expand the functional repertoire of the precursor pVII protein in lytic HAdV-C5 infection and highlight MKRN1 as a common target protein during different virus infections.

MATERIALS AND METHODS

Plasmids, siRNAs, and cell lines. Human MKRN1 (NM_013446) GenEZ ORF clone (GenScript, Inc.) was cloned into pcDNA3.1-HA and pcDNA3.1-Flag plasmids to express HA- and Flag-tagged MKRN1 proteins. In the same plasmid background, an MKRN1 point mutant (H307E) and deletion mutants (1-267, 112-267, and 112-482) were generated using a QuikChange Lightning site-directed mutagenesis kit (Agilent Technologies) and PCR-mediated DNA deletion, respectively. To express the GST-MKRN1 proteins, the wild-type (1-482), point mutant (H307E), and deletion mutant (1-267) sequences were cloned into the pGEX-6P-1 (GE Healthcare Life Sciences) plasmid. The plasmid expressing Flag-E1B55K was generated by recloning the HAdV-C2 E1B55K cDNA from the pCMVE1B55K plasmid (60) into the pcDNA3.1-Flag plasmid. The plasmids expressing HAdV-C5 Flag-E4orf6 (61) and 6×His-ubiquitin (62) were kindly provided by Paola Blanchette and Dimitris Xirodimas, respectively. The plasmids encoding codon-optimized GST-pVII(wt), GST-pVII(Δ24), pVII(wt)-Flag, and pVII(Δ24)-Flag proteins have been described before (12).

The H1299, HEK293, A549, 911, and U2OS cell lines were originally obtained from the American Type Culture Collection (ATCC). All cell lines were grown in Dulbecco's modified Eagle medium (DMEM; Invitrogen) supplemented with 10% fetal calf serum (FCS; PAA) and penicillin-streptomycin (PEST) solution (Gibco) in a 7% CO_2-containing cell incubator. A stable HeLa cell line expressing codon-optimized pVII(wt)-Flag was generated using the Flp-In recombination system in the HeLa-Flp-In T-Rex cell line (63). All transfections were performed using Turbofect transfection reagent (Thermo Scientific) according to the manufacturer's instructions.

HAdV infections. The following viruses were used: wild-type HAdV-C5 (generously provided by Göran Akusjärvi) and E1B55K-deficient HAdV-C2 (dl1520) (54). Replication-competent HAdV-C5 expressing the pVII-Flag fusion protein (HAdV-pVII-Flag) was generated using pTG3602 as background viral DNA (64). The pTG3602 plasmid was cotransformed with linearized donor DNA containing the HAdV-C5 pVII sequence fused in-frame with the Flag epitope tag sequence and chloramphenicol resistance gene into *Escherichia coli* BJ5183 cells (Agilent Technologies). Following the recombination, the positive clones were selected with chloramphenicol and analyzed by PCR and sequencing. After removal of the chloramphenicol resistance gene with SwaI restriction enzyme cleavage, the plasmid was amplified and cleaved with PacI restriction enzyme to remove the ampicillin resistance gene. Finally, the PacI-linearized plasmid was transfected into HEK293 cells using Turbofect reagent. The HAdV-pVII-Flag virus was amplified in 911 cells and purified by CsCl gradient centrifugation. Virus infections and titrations were

done as described previously (65). The multiplicity of infection (MOI) (fluorescence-forming units [FFU]/per cell) is indicated in the respective figure legends.

Other virus infections. For HCV, Huh7.5 cells were infected in 12-well plates for 48 h using the HCV genotype 2a strain clone pFK-JFH1/J6/C-846-dg (pFK-JC1) at an MOI of 0.5. Cells were lysed in lysis buffer (0.5% NP-40, 5 M NaCl, 0.5 mM EDTA, 1 M Tris-HCl [pH 7.5], 0.075g EGTA, 1% Triton X-100, 10% glycerol, 10 mM $Na_4P_2O_7$ in 50 ml) containing cOmplete protease inhibitors (Roche). For HBV, HepaRG cells were cultured in Williams medium containing 10% FCS (ThermoFisher Scientific) and 1% PEST, 1% nonessential amino acids, 2 mmol/liter L-glutamine, and 1% of sodium pyruvate (all from GIBCO), Insuman Rapid insulin (Sanofi Aventis), gentamicin (Ratiopharm), and hydrocortisone (Pfizer, Inc.). For differentiation, 1.8% of dimethyl sulfoxide (DMSO) was added to the growth medium. HepaRG cells were differentiated for a time period of 4 weeks. Infection was carried out by using HBV at an MOI of 200 for 24 h and washing the cells the following day. Cells were lysed as indicated above at 12 days postinfection. For MV, Vero cells were plated in 12-well plates and infected with rMVrEdt-eGFP (kindly provided by Bert Rima, [66] and Jürgen Schneider-Schaulies) at an MOI of 0.1. Cells were lysed 48 hpi as indicated above. For VSV, Huh7.5 cells were plated in 12-well plates and infected with VSV*ΔG(LCMVgp) at an MOI of 0.6 (kind gift of Gert Zimmer [67]). Cells were lysed 18 hpi as indicated above. Since both MVeGFP and VSV*ΔG(LCMVgp) express GFP, the infections were confirmed with fluorescence monitoring by using a CKX41 inverted microscope (Olympus) with an LCachN/10×/0.40 Phc/1/FN22 UIS objective (data not shown). For HIV-1, LC5-RIC cells were infected with HIV-1 LAI infectious molecular clone (pLAI.2) (68) and lysed 48 hpi as indicated above.

Antibodies and chemicals. The following primary antibodies were used: anti-mouse Flag (Sigma; M2, F1804), anti-rabbit Flag (Sigma; F7425), anti-rabbit HA (Santa Cruz; sc-805), anti-rabbit HMGB2 (Abcam; ab67282), anti-mouse C1QBP (Santa Cruz; sc-23885), anti-rabbit MKRN1 (Bethyl Laboratories; A300-990A), anti-rabbit SET (Novus Biologicals; NBP1-30888), anti-rabbit ACF1(BAZ1A) (Novus Biologicals; NB100-61042), anti-rabbit CHD3 (Novus Biologicals; NB100-60412), anti-mouse GAPDH (Ambion, Am4300), anti-mouse Mre11 (Abcam, ab214), anti-mouse His (Clontech, 631212), anti-mouse ubiquitin (FK2; Enzo BML-PW8810), anti-goat actin (Santa Cruz; sc-1616), anti-rabbit GST (Santa Cruz; sc-33614), anti-mouse E1A (EMD Millipore; DP11-UG100), anti-mouse E1B55K (2A6 [69]), anti-rabbit GFP (Clontech; 632376), anti-HCV core, anti-mouse HIV-1 p24 (Chemicon International; MAB880-A), anti-rabbit measles virus nucleoprotein NP (Covalab; pab0035), and anti-rabbit HAdV-5 Capsid (Abcam; ab6982). To inhibit proteasome, MG132 (Sigma; C2211, dissolved in DMSO) was used at a final concentration of 25 μM for 4 h unless otherwise specified in the figure legends. Control cells were treated only with DMSO. To inhibit protein synthesis, cells were treated with cycloheximide (Sigma; C4859, dissolved in DMSO) at a final concentration of 100 μg/ml.

Yeast two-hybrid analysis. Yeast two-hybrid screening was performed by Hybrigenics Services, S.A.S., Paris, France. The codon-optimized coding sequence for HAdV-C5 pVII (12) was PCR amplified and cloned into the pB29 vector as an N-terminal fusion to LexA (N-pVII-LexA-C). The generated construct was used as bait to screen a random-primed human lung cancer cDNA library constructed into the pP6 vector. A total of 104 million clones (10-fold the complexity of the library) were screened using a mating approach with YHGX13 (Y187 *ade2-101::loxP-kanMX-loxP matα*) and L40ΔGal4 (*matα*) yeast strains as previously described (70). Two hundred fifty-three His$^+$ colonies were selected on a medium lacking tryptophan, leucine, and histidine. The prey fragments of the positive clones were amplified by PCR and sequenced at their 5′ and 3′ junctions to identify the corresponding interacting proteins in the GenBank database (NCBI). A confidence score (predicted biological score [PBS]) was attributed to each interaction. The PBS relies on two different levels of analysis. First, a local score takes into account the redundancy and independence of prey fragments as well as the distribution of reading frames and stop codons in overlapping fragments. Second, a global score takes into account the interactions found in all the screens performed at Hybrigenics using the same library. This global score represents the probability of an interaction being nonspecific. For practical use, the scores are divided into four categories, from A (highest confidence) to D (lowest confidence).

In situ PLA. A proximity ligation assay (PLA) was carried out using reagents and instructions from a Duolink II kit (Olink Biosciences). Briefly, the HeLa-pVII(wt)-Flag cells were treated with doxycycline (final concentration, 0.2 μg/ml) to induce pVII(wt)-Flag protein expression (71). Thirty-six hours postinduction, the cells were washed twice with phosphate-buffered saline, fixed with 3% paraformaldehyde for 15 min, and permeabilized with 0.05% Triton in phosphate-buffered saline for 15 min at room temperature. After the cells were blocked with Duolink II blocking solution overnight at 4°C, the slides were incubated with primary antibodies in a humidity chamber for 1 h. Due to the antibody specificity requirement in the PLA assay, the anti-mouse Flag antibody was combined with anti-rabbit antibodies (HMGB2, MKRN1, SET, BAZ1A, CHD3). An exception was anti-mouse C1QBP antibody, which was combined with anti-rabbit Flag antibody. The slides were washed three times, 5 min each time, with TBS-T (Tris-buffered saline plus 0.05% Tween 20) prior to incubation with anti-mouse and anti-rabbit secondary probes (Duolink II) for 90 min at 37°C. The ligation solution containing the Duolink ligase (Duolink II) was applied to the TBS-T-washed slides for 30 min at 37°C. Further, the slides were washed with TBS-T, and 40 μl of amplification solution was added to each sample and incubated in a preheated humidity chamber for 90 min at 37°C. Thereafter, the slides were washed once in TBS, stained with Hoechst dye, and mounted with 10 μl SlowFade mounting medium (Life Technologies). Labeled cells were visualized with a Zeiss AxioPlan2 epi-microscope. Image analysis and signal quantification were performed with the Duolink ImageTool software (Olink Bioscience).

Cell lysates and Western blotting. In general, cells were lysed in radioimmunoprecipitation assay (RIPA) buffer (12) for 20 min on ice, sonicated, and centrifuged at 15,000 rpm and 4°C for 15 min. When

the whole-cell lysates were prepared from H1299 cells expressing the Flag-E1B55K and Flag-E4orf6 proteins (Fig. 4), the whole-cell lysates were made as described in reference 61. Western blot membranes, either nitrocellulose or polyvinylidene difluoride (PVDF), were incubated with primary antibodies overnight at 4°C, followed by incubation with the fluorescent-labeled secondary antibodies (IRDye; LI-COR). The membranes were scanned using an Odyssey scanner (LI-COR), and the protein signals were quantified using Image Studio Software (LI-COR) (12).

Immunoprecipitation. Approximately 8×10^6 H1299 cells were either transfected or infected with HAdV-pVII-Flag virus. The cells were lysed in lysis buffer (150 mM NaCl, 1 mM EDTA, 0.5% NP-40, 0.5% Triton X-100, 0.1% sodium deoxycholate, 50 mM Tris-HCl [pH 7.5], 1 mM dithiothreitol [DTT], and cOmplete protease inhibitors [Roche]) for 30 min at 4°C. The soluble cell lysates were incubated with an anti-Flag (M2)-coupled Sepharose beads (Sigma) for 2 h at 4°C. The beads were washed three times in 1 ml of lysis buffer, and bound proteins were eluted with 2× SDS loading dye and separated by SDS-PAGE.

GST pulldown assay. The GST pulldown assay was done as described previously (12). Approximately 2 μg of glutathione Sepharose bead-bound GST and GST-pVII(wt or Δ24) proteins were incubated with H1299 whole-cell lysates expressing the Flag-MKRN1(1-482), HA-MKRN1(1-482), HA-MKRN1(1-267), HA-MKRN1(112-267), and HA-MKRN1(112-482) proteins at room temperature for 1 h. The beads were washed extensively with washing buffer (25 mM HEPES-KOH [pH 7.4], 12.5 mM MgCl$_2$, 200 mM KCl, 0.1 mM EDTA, 10% glycerol, 0.1% NP-40). The bound proteins were separated on 12% SDS-PAGE, followed by detection by Western blotting.

GST-MKRN1 purification. BL21(DE3)-RIPL cells (Agilent Technologies) transformed with pGEX-6P-MKRN1(wt), pGEX-6P-MKRN1(1-267), and pGEX-6P-MKRN1(H307E) were grown at 37°C in LB medium to an optical density at 600 nm (OD$_{600}$) of 0.5 to 0.6. Protein expression was induced with 1 mM IPTG (isopropyl-β-D-thiogalactopyranoside) for 4 h at 37°C. The cell pellets were lysed in lysis buffer (50 mM Tris-HCl [pH 7.5], 150 mM NaCl, 0.05% NP-40, 1 mM DTT, 0.25 mg lysozyme, and protease inhibitors). Cell lysates were sonicated, filtered through a 0.45-μm filter, and purified using a GSTrap FF column (GE Healthcare) in an ÄKTAxpress system (GE Healthcare) according to the manufacturer's recommendations. The column was equilibrated and washed in washing buffer (50 mM Tris-HCl [pH 7.5], 150 mM NaCl), and the proteins were eluted in washing buffer supplemented with 10 mM reduced glutathione (Sigma). Purified proteins were dialyzed against storage buffer (phosphate-buffered saline plus 20% glycerol).

In vivo ubiquitination assay. The in vivo ubiquitination experiments were performed as described before (62). Briefly, H1299 cells were transfected with plasmids expressing the HA-MKRN1(wt), HA-MKRN1(1-267), HA-MKRN1(H307E), 6×His-ubiquitin, pVII(wt)-Flag, and pVII(Δ24)-Flag proteins. Thirty-six hours posttransfection, the cells were treated with MG132 (10 μM, 4 h), followed by cell lysis in buffer containing 6 M guanidine, 10 mM β-mercaptoethanol, 5 mM N-ethylmaleimide, and 5 mM imidazole. The cell lysates were incubated with nickel-coupled agarose beads (Ni-nitrilotriacetic acid [Ni-NTA] beads, Qiagen) by rotation at 4°C overnight. The beads were washed with buffer containing 8 M urea, 10 mM β-mercaptoethanol, and 0.1% NP-40. Finally, the proteins were eluted from the Ni-NTA beads with a sample buffer containing 0.72 M β-mercaptoethanol and 200 mM imidazole.

In vitro ubiquitination assay. Equal amounts of the purified GST-MKRN1 proteins (wt, H307E, and 1-267) were mixed with purified His-UbE1, His-UbcH5a, and Ubiquitin-MAX proteins (all from Viva Biosciences) in a reaction buffer containing 40 mM Tris-HCl [pH 7.5], 1 mM DTT, 5 mM MgCl$_2$, and 2 mM ATP according to the manufacturer's recommendations. After incubation at 37°C for 2 h, reactions were terminated with 2× SDS loading dye.

RNA extraction and qRT-PCR. Total RNA extraction, cDNA synthesis with random primers, and reverse transcription-quantitative PCRs (qRT-PCRs) were performed as previously described (65). The following MKRN1 primers were used: tp575 (5'-GCAGCAAGGGATGACTTTGT-3') and tp576 (5'-TGTATTTA TGGAGACCGCTGC-3'). Relative levels of MKRN1 mRNA expression were calculated after normalization to the HPRT1 mRNA levels using the $2^{-\Delta\Delta C_T}$ method (72).

REFERENCES

1. Lion T. 2014. Adenovirus infections in immunocompetent and immuno-compromised patients. Clin Microbiol Rev 27:441–462. https://doi.org/10.1128/CMR.00116-13.

2. Assadian F, Sandstrom K, Bondeson K, Laurell G, Lidian A, Svensson C, Akusjarvi G, Bergqvist A, Punga T. 2016. Distribution and molecular characterization of human adenovirus and Epstein-Barr virus infections in tonsillar lymphocytes isolated from patients diagnosed with tonsillar diseases. PLoS One 11:e0154814. https://doi.org/10.1371/journal.pone.0154814.

3. Russell WC. 2009. Adenoviruses: update on structure and function. J Gen Virol 90:1–20. https://doi.org/10.1099/vir.0.003087-0.

4. Alestrom P, Akusjarvi G, Lager M, Yeh-kai L, Pettersson U. 1984. Genes encoding the core proteins of adenovirus type 2. J Biol Chem 259:13980–13985.

5. Benevento M, Di Palma S, Snijder J, Moyer CL, Reddy VS, Nemerow GR, Heck AJ. 2014. Adenovirus composition, proteolysis, and disassembly studied by in-depth qualitative and quantitative proteomics. J Biol Chem 289:11421–11430. https://doi.org/10.1074/jbc.M113.537498.

6. Blainey PC, Graziano V, Perez-Berna AJ, McGrath WJ, Flint SJ, San Martin C, Xie XS, Mangel WF. 2013. Regulation of a viral proteinase by a peptide and DNA in one-dimensional space: IV. Viral proteinase slides along DNA to locate and process its substrates. J Biol Chem 288:2092–2102. https://doi.org/10.1074/jbc.M112.407460.

7. Ruzindana-Umunyana A, Imbeault L, Weber JM. 2002. Substrate speci-ficity of adenovirus protease. Virus Res 89:41–52. https://doi.org/10.1016/S0168-1702(02)00111-9.

8. Sung MT, Cao TM, Lischwe MA, Coleman RT. 1983. Molecular processing of adenovirus proteins. J Biol Chem 258:8266–8272.

9. Webster A, Russell S, Talbot P, Russell WC, Kemp GD. 1989. Character-ization of the adenovirus proteinase: substrate specificity. J Gen Virol 70:3225–3234. https://doi.org/10.1099/0022-1317-70-12-3225.

10. Ortega-Esteban A, Condezo GN, Perez-Berna AJ, Chillon M, Flint SJ, Reguera D, San Martin C, de Pablo PJ. 2015. Mechanics of viral chromatin reveals the pressurization of human adenovirus. ACS Nano 9:10826–10833. https://doi.org/10.1021/acsnano.5b03417.

11. Perez-Berna AJ, Marion S, Chichon FJ, Fernandez JJ, Winkler DC, Carras-cosa JL, Steven AC, Siber A, San Martin C. 2015. Distribution of DNA-condensing protein complexes in the adenovirus core. Nucleic Acids Res 43:4274–4283. https://doi.org/10.1093/nar/gkv187.

12. Inturi R, Thaduri S, Punga T. 2013. Adenovirus precursor pVII protein stability is regulated by its propeptide sequence. PLoS One 8:e80617. https://doi.org/10.1371/journal.pone.0080617.

13. Chatterjee PK, Vayda ME, Flint SJ. 1986. Adenoviral protein VII packages intracellular viral DNA throughout the early phase of infection. EMBO J 5:1633–1644.

14. Lischwe MA, Sung MT. 1977. A histone-like protein from adenovirus chromatin. Nature 267:552–554. https://doi.org/10.1038/267552a0.

15. Vayda ME, Rogers AE, Flint SJ. 1983. The structure of nucleoprotein cores released from adenovirions. Nucleic Acids Res 11:441–460. https://doi.org/10.1093/nar/11.2.441.

16. Corden J, Engelking HM, Pearson GD. 1976. Chromatin-like organization of the adenovirus chromosome. Proc Natl Acad Sci U S A 73:401–404. https://doi.org/10.1073/pnas.73.2.401.

17. Ostapchuk P, Suomalainen M, Zheng Y, Boucke K, Greber UF, Hearing P. 2017. The adenovirus major core protein VII is dispensable for virion assembly but is essential for lytic infection. PLoS Pathog 13:e1006455. https://doi.org/10.1371/journal.ppat.1006455.

18. Komatsu T, Dacheux D, Kreppel F, Nagata K, Wodrich H. 2015. A method for visualization of incoming adenovirus chromatin complexes in fixed and living cells. PLoS One 10:e0137102. https://doi.org/10.1371/journal.pone.0137102.

19. Wodrich H, Cassany A, D'Angelo MA, Guan T, Nemerow G, Gerace L. 2006. Adenovirus core protein pVII is translocated into the nucleus by multiple import receptor pathways. J Virol 80:9608–9618. https://doi.org/10.1128/JVI.00850-06.

20. Cassany A, Ragues J, Guan T, Begu D, Wodrich H, Kann M, Nemerow GR, Gerace L. 2015. Nuclear import of adenovirus DNA involves direct inter-action of hexon with an N-terminal domain of the nucleoporin Nup214. J Virol 89:1719–1730. https://doi.org/10.1128/JVI.02639-14.

21. Karen KA, Hearing P. 2011. Adenovirus core protein VII protects the viral genome from a DNA damage response at early times after infection. J Virol 85:4135–4142. https://doi.org/10.1128/JVI.02540-10.

22. Komatsu T, Haruki H, Nagata K. 2011. Cellular and viral chromatin proteins are positive factors in the regulation of adenovirus gene ex-pression. Nucleic Acids Res 39:889–901. https://doi.org/10.1093/nar/gkq783.

23. Komatsu T, Nagata K. 2012. Replication-uncoupled histone deposition during adenovirus DNA replication. J Virol 86:6701–6711. https://doi.org/10.1128/JVI.00380-12.

24. Haruki H, Okuwaki M, Miyagishi M, Taira K, Nagata K. 2006. Involvement of template-activating factor I/SET in transcription of adenovirus early genes as a positive-acting factor. J Virol 80:794–801. https://doi.org/10.1128/JVI.80.2.794-801.2006.

25. Matsumoto K, Okuwaki M, Kawase H, Handa H, Hanaoka F, Nagata K. 1995. Stimulation of DNA transcription by the replication factor from the adenovirus genome in a chromatin-like structure. J Biol Chem 270:9645–9650. https://doi.org/10.1074/jbc.270.16.9645.

26. Okuwaki M, Nagata K. 1998. Template activating factor-I remodels the chromatin structure and stimulates transcription from the chromatin template. J Biol Chem 273:34511–34518. https://doi.org/10.1074/jbc.273.51.34511.

27. Johnson JS, Osheim YN, Xue Y, Emanuel MR, Lewis PW, Bankovich A, Beyer AL, Engel DA. 2004. Adenovirus protein VII condenses DNA, represses transcription, and associates with transcriptional activator E1A. J Virol 78:6459–6468. https://doi.org/10.1128/JVI.78.12.6459-6468.2004.

28. Avgousti DC, Herrmann C, Kulej K, Pancholi NJ, Sekulic N, Petrescu J, Molden RC, Blumenthal D, Paris AJ, Reyes ED, Ostapchuk P, Hearing P, Seeholzer SH, Worthen GS, Black BE, Garcia BA, Weitzman MD. 2016. A core viral protein binds host nucleosomes to sequester immune danger signals. Nature 535:173–177. https://doi.org/10.1038/nature18317.

29. Avgousti DC, Della Fera AN, Otter CJ, Herrmann C, Pancholi NJ, Weitz-man MD. 9 August 2017. Adenovirus core protein VII down-regulates the DNA damage response on the host genome. J Virol https://doi.org/10.1128/JVI.01089-17.

30. Chondrogianni N, Gonos ES. 2012. Structure and function of the ubiquitin-proteasome system: modulation of components. Prog Mol Biol Transl Sci 109:41–74. https://doi.org/10.1016/B978-0-12-397863-9.00002-X.

31. Blanchette P, Branton PE. 2009. Manipulation of the ubiquitin-proteasome pathway by small DNA tumor viruses. Virology 384:317–323. https://doi.org/10.1016/j.virol.2008.10.005.

32. Schreiner S, Wimmer P, Dobner T. 2012. Adenovirus degradation of cellular proteins. Future Microbiol 7:211–225. https://doi.org/10.2217/fmb.11.153.

33. Wimmer P, Schreiner S. 2015. Viral mimicry to usurp ubiquitin and SUMO host pathways. Viruses 7:4854–4872. https://doi.org/10.3390/v7092849.

34. Baker A, Rohleder KJ, Hanakahi LA, Ketner G. 2007. Adenovirus E4 34k and E1b 55k oncoproteins target host DNA ligase IV for proteasomal degradation. J Virol 81:7034–7040. https://doi.org/10.1128/JVI.00029-07.

35. Dallaire F, Blanchette P, Groitl P, Dobner T, Branton PE. 2009. Identifica-tion of integrin alpha3 as a new substrate of the adenovirus E4orf6/E1B 55-kilodalton E3 ubiquitin ligase complex. J Virol 83:5329–5338. https://doi.org/10.1128/JVI.00089-09.

36. Gupta A, Jha S, Engel DA, Ornelles DA, Dutta A. 2013. Tip60 degradation by adenovirus relieves transcriptional repression of viral transcriptional activator EIA. Oncogene 32:5017–5025. https://doi.org/10.1038/onc.2012.534.

37. Querido E, Blanchette P, Yan Q, Kamura T, Morrison M, Boivin D, Kaelin WG, Conaway RC, Conaway JW, Branton PE. 2001. Degradation of p53 by adenovirus E4orf6 and E1B55K proteins occurs via a novel mechanism involving a Cullin-containing complex. Genes Dev 15:3104–3117. https://doi.org/10.1101/gad.926401.

38. Schreiner S, Burck C, Glass M, Groitl P, Wimmer P, Kinkley S, Mund A, Everett RD, Dobner T. 2013. Control of human adenovirus type 5 gene expression by cellular Daxx/ATRX chromatin-associated complexes. Nu-cleic Acids Res 41:3532–3550. https://doi.org/10.1093/nar/gkt064.

39. Schreiner S, Kinkley S, Burck C, Mund A, Wimmer P, Schubert T, Groitl P, Will H, Dobner T. 2013. SPOC1-mediated antiviral host cell response is antagonized early in human adenovirus type 5 infection. PLoS Pathog 9:e1003775. https://doi.org/10.1371/journal.ppat.1003775.

40. Stracker TH, Carson CT, Weitzman MD. 2002. Adenovirus oncoproteins

inactivate the Mre11-Rad50-NBS1 DNA repair complex. Nature 418: 348–352. https://doi.org/10.1038/nature00863.

41. Gray TA, Hernandez L, Carey AH, Schaldach MA, Smithwick MJ, Rus K, Marshall Graves JA, Stewart CL, Nicholls RD. 2000. The ancient source of a distinct gene family encoding proteins featuring RING and C(3)H zinc-finger motifs with abundant expression in developing brain and nervous system. Genomics 66:76–86. https://doi.org/10.1006/geno.2000.6199.

42. Kim JH, Park SM, Kang MR, Oh SY, Lee TH, Muller MT, Chung IK. 2005. Ubiquitin ligase MKRN1 modulates telomere length homeostasis through a proteolysis of hTERT. Genes Dev 19:776–781. https://doi.org/10.1101/gad.1289405.

43. Kim JH, Park KW, Lee EW, Jang WS, Seo J, Shin S, Hwang KA, Song J. 2014. Suppression of PPARgamma through MKRN1-mediated ubiquiti-nation and degradation prevents adipocyte differentiation. Cell Death Differ 21:594–603. https://doi.org/10.1038/cdd.2013.181.

44. Ko A, Shin JY, Seo J, Lee KD, Lee EW, Lee MS, Lee HW, Choi IJ, Jeong JS, Chun KH, Song J. 2012. Acceleration of gastric tumorigenesis through MKRN1-mediated posttranslational regulation of p14ARF. J Natl Cancer Inst 104:1660–1672. https://doi.org/10.1093/jnci/djs424.

45. Lee EW, Kim JH, Ahn YH, Seo J, Ko A, Jeong M, Kim SJ, Ro JY, Park KM, Lee HW, Park EJ, Chun KH, Song J. 2012. Ubiquitination and degradation of the FADD adaptor protein regulate death receptor-mediated apop-tosis and necroptosis. Nat Commun 3:978. https://doi.org/10.1038/ncomms1981.

46. Lee EW, Lee MS, Camus S, Ghim J, Yang MR, Oh W, Ha NC, Lane DP, Song J. 2009. Differential regulation of p53 and p21 by MKRN1 E3 ligase controls cell cycle arrest and apoptosis. EMBO J 28:2100–2113. https://doi.org/10.1038/emboj.2009.164.

47. Lee MS, Jeong MH, Lee HW, Han HJ, Ko A, Hewitt SM, Kim JH, Chun KH, Chung JY, Lee C, Cho H, Song J. 2015. PI3K/AKT activation induces PTEN ubiquitination and destabilization accelerating tumourigenesis. Nat Commun 6:7769. https://doi.org/10.1038/ncomms8769.

48. Ko A, Lee EW, Yeh JY, Yang MR, Oh W, Moon JS, Song J. 2010. MKRN1 induces degradation of West Nile virus capsid protein by functioning as an E3 ligase. J Virol 84:426–436. https://doi.org/10.1128/JVI.00725-09.

49. Finsterbusch T, Steinfeldt T, Doberstein K, Rodner C, Mankertz A. 2009. Interaction of the replication proteins and the capsid protein of porcine circovirus type 1 and 2 with host proteins. Virology 386:122–131. https://doi.org/10.1016/j.virol.2008.12.039.

50. Cassar PA, Carpenedo RL, Samavarchi-Tehrani P, Olsen JB, Park CJ, Chang WY, Chen Z, Choey C, Delaney S, Guo H, Guo H, Tanner RM, Perkins TJ, Tenenbaum SA, Emili A, Wrana JL, Gibbings D, Stanford WL. 2015. Integrative genomics positions MKRN1 as a novel ribonucleoprotein within the embryonic stem cell gene regulatory network. EMBO Rep 16:1334–1357. https://doi.org/10.15252/embr.201540974.

51. Omwancha J, Zhou XF, Chen SY, Baslan T, Fisher CJ, Zheng Z, Cai C, Shemshedini L. 2006. Makorin RING finger protein 1 (MKRN1) has neg-ative and positive effects on RNA polymerase II-dependent transcription. Endocrine 29:363–373. https://doi.org/10.1385/ENDO:29:2:363.

52. Haruki H, Gyurcsik B, Okuwaki M, Nagata K. 2003. Ternary complex formation between DNA-adenovirus core protein VII and TAF-Ibeta/SET, an acidic molecular chaperone. FEBS Lett 555:521–527. https://doi.org/10.1016/S0014-5793(03)01336-X.

53. Xue Y, Johnson JS, Ornelles DA, Lieberman J, Engel DA. 2005. Adenovirus protein VII functions throughout early phase and interacts with cellular proteins SET and pp32. J Virol 79:2474–2483. https://doi.org/10.1128/JVI.79.4.2474-2483.2005.

54. Barker DD, Berk AJ. 1987. Adenovirus proteins from both E1B reading frames are required for transformation of rodent cells by viral infection and DNA transfection. Virology 156:107–121. https://doi.org/10.1016/0042-6822(87)90441-7.

55. Miroci H, Schob C, Kindler S, Olschlager-Schutt J, Fehr S, Jungenitz T, Schwarzacher SW, Bagni C, Mohr E. 2012. Makorin ring zinc finger

protein 1 (MKRN1), a novel poly(A)-binding protein-interacting protein, stimulates translation in nerve cells. J Biol Chem 287:1322–1334. https://doi.org/10.1074/jbc.M111.315291.

56. Torchy MP, Hamiche A, Klaholz BP. 2015. Structure and function insights into the NuRD chromatin remodeling complex. Cell Mol Life Sci 72: 2491–2507. https://doi.org/10.1007/s00018-015-1880-8.

57. Lans H, Marteijn JA, Vermeulen W. 2012. ATP-dependent chromatin remodeling in the DNA-damage response. Epigenetics Chromatin 5:4. https://doi.org/10.1186/1756-8935-5-4.

58. Bergstrom Lind S, Artemenko KA, Elfineh L, Zhao Y, Bergquist J, Pet-tersson U. 2012. The phosphoproteome of the adenovirus type 2 virion. Virology 433:253–261. https://doi.org/10.1016/j.virol.2012.08.012.

59. Liu L, Oliveira NM, Cheney KM, Pade C, Dreja H, Bergin AM, Borgdorff V, Beach DH, Bishop CL, Dittmar MT, McKnight A. 2011. A whole genome screen for HIV restriction factors. Retrovirology 8:94. https://doi.org/10.1186/1742-4690-8-94.

60. Punga T, Akusjarvi G. 2003. Adenovirus 2 E1B-55K protein relieves p53-mediated transcriptional repression of the survivin and MAP4 promoters. FEBS Lett 552:214–218. https://doi.org/10.1016/S0014-5793(03)00927-X.

61. Cheng CY, Gilson T, Dallaire F, Ketner G, Branton PE, Blanchette P. 2011. The E4orf6/E1B55K E3 ubiquitin ligase complexes of human adenovi-ruses exhibit heterogeneity in composition and substrate specificity. J Virol 85:765–775. https://doi.org/10.1128/JVI.01890-10.

62. Xirodimas D, Saville MK, Edling C, Lane DP, Lain S. 2001. Different effects of p14ARF on the levels of ubiquitinated p53 and Mdm2 in vivo. Oncogene 20:4972–4983. https://doi.org/10.1038/sj.onc.1204656.

63. Hewitt L, Tighe A, Santaguida S, White AM, Jones CD, Musacchio A, Green S, Taylor SS. 2010. Sustained Mps1 activity is required in mitosis to recruit O-Mad2 to the Mad1-C-Mad2 core complex. J Cell Biol 190:25–34. https://doi.org/10.1083/jcb.201002133.

64. Chartier C, Degryse E, Gantzer M, Dieterle A, Pavirani A, Mehtali M. 1996. Efficient generation of recombinant adenovirus vectors by homologous recombination in Escherichia coli. J Virol 70:4805–4810.

65. Inturi R, Kamel W, Akusjarvi G, Punga T. 2015. Complementation of the human adenovirus type 5 VA RNAi defect by the vaccinia virus E3L protein and serotype-specific VA RNAis. Virology 485:25–35. https://doi.org/10.1016/j.virol.2015.07.002.

66. Duprex WP, McQuaid S, Roscic-Mrkic B, Cattaneo R, McCallister C, Rima BK. 2000. In vitro and in vivo infection of neural cells by a recombinant measles virus expressing enhanced green fluorescent protein. J Virol 74:7972–7979. https://doi.org/10.1128/JVI.74.17.7972-7979.2000.

67. Berger Rentsch M, Zimmer G. 2011. A vesicular stomatitis virus replicon-based bioassay for the rapid and sensitive determination of multi-species type I interferon. PLoS One 6:e25858. https://doi.org/10.1371/journal.pone.0025858.

68. Kremb S, Helfer M, Heller W, Hoffmann D, Wolff H, Kleinschmidt A, Cepok S, Hemmer B, Durner J, Brack-Werner R. 2010. EASY-HIT: HIV full-replication technology for broad discovery of multiple classes of HIV inhibitors. Antimicrob Agents Chemother 54:5257–5268. https://doi.org/10.1128/AAC.00515-10.

69. Sarnow P, Sullivan CA, Levine AJ. 1982. A monoclonal antibody detecting the adenovirus type 5-E1b-58Kd tumor antigen: characterization of the E1b-58Kd tumor antigen in adenovirus-infected and -transformed cells. Virology 120:510–517. https://doi.org/10.1016/0042-6822(82)90054-X.

70. Fromont-Racine M, Rain JC, Legrain P. 1997. Toward a functional analysis of the yeast genome through exhaustive two-hybrid screens. Nat Genet 16:277–282. https://doi.org/10.1038/ng0797-277.

71. Krzywkowski T, Ciftci S, Assadian F, Nilsson M, Punga T. 2017. Simulta-neous single-cell in situ analysis of human adenovirus type 5 DNA and mRNA expression patterns in lytic and persistent infection. J Virol 91: e00166-17. https://doi.org/10.1128/JVI.00166-17.

72. Schmittgen TD, Livak KJ. 2008. Analyzing real-time PCR data by the comparative C(T) method. Nat Protoc 3:1101–1108. https://doi.org/10.1038/nprot.2008.73.